

# Investigating the Impact of Randomness on Reproducibility in Computer Vision: A Study on Applications in Civil Engineering and Medicine

Bahadır Eryılmaz      Osman Alperen Koraş      Jörg Schlötterer      Christin Seifert  
University Hospital Essen      University Hospital Essen      University of Marburg & of Mannheim      University of Marburg  
Essen, Germany      Essen, Germany      Marburg & Mannheim, Germany      Marburg, Germany  
0009-0002-8743-4751      0009-0006-6490-3139      0000-0002-3678-0390      0000-0002-6776-3868

**Abstract**—Reproducibility is essential for scientific research. However, in computer vision, achieving consistent results is challenging due to various factors. One influential, yet often unrecognized, factor is CUDA-induced randomness. Despite CUDA’s advantages for accelerating algorithm execution on GPUs, if not controlled, its behavior across multiple executions remains non-deterministic. While reproducibility issues in ML being researched, the implications of CUDA-induced randomness in application are yet to be understood. Our investigation focuses on this randomness across one standard benchmark dataset and two real-world datasets in an isolated environment. Our results show that CUDA-induced randomness can account for differences up to 4.77% in performance scores. We find that managing this variability for reproducibility may entail increased runtime or reduce performance, but that disadvantages are not as significant as reported in previous studies.

**Index Terms**—deep learning, reproducibility, randomness, computer vision, determinism

## I. INTRODUCTION

The reproducibility crisis in machine learning is a growing concern that questions the reliability and validity of reported research findings [1]. One survey shows that not all researchers are aware of this problem [2]. This issue stems from the difficulty in replicating results due to various unknown and poorly understood factors, including but not limited to differences in data preparation, algorithmic details and computational environments. Deep learning architectures, as they are widely used in computer vision, with their complex, multi-layered neural networks [3], further impede reproducibility, as these models often involve numerous hyperparameters and training details that can lead to significant variability in results.

However, even in tightly controlled training environments, different training runs can lead to models with different weights and performances due to CUDA-induced randomness [4] caused by non-deterministic implementations of certain operations, differences in floating-point arithmetic precision, and the parallel execution order of operations, which may not be consistent across runs or different hardware setups.

This study was funded by a PhD grant from the DFG Research Training Group 2535 Knowledge-and data-based personalization of medicine at the point of care (WisPerMed).

While it is possible to compare the performance of different modes on an appropriate evaluation dataset, the significance of such comparisons is limited to the specific checkpoints evaluated. The presence of CUDA-induced randomness, alongside other sources, complicates the attribution of performance differences between models to their architectural or algorithmic differences, since random factors alone can account for significant variances in scores [5]. To conclusively assess whether one machine learning algorithm outperforms another, it would be necessary to train multiple models to sample the space induced by that algorithm [2]. However, this approach is often impractical for a single study, especially given the trend towards larger models that demand increasing substantial computational resources.

Despite these concerns, the runtime improvements gained through the parallelization capabilities of CUDA GPUs indicates that their use will remain indispensable in the foreseeable future [6], [7]. This reality emphasizes the importance of understanding CUDA-induced randomness and its impact on model performance in real-world applications. After all, a lack of such insight could lead researchers to overestimate or underestimate the capabilities of machine learning algorithms, which in turn could misdirect the efforts of the research community.

We investigate the effects of CUDA-induced randomness, its implications on reproducibility, and its broader implications on real-world computer vision applications.

## II. RELATED WORK

Goodman et al. [8] provide a foundational definition of reproducibility, framing the standards we adopted in our study. Raste et al. [9] analyzed the effects of randomness in model training and dataset partitioning, but did not investigate CUDA randomness in their setup. Chen et al. [10] detail the challenges inherent in reproducing deep learning results and showcase their solutions through empirical case studies. The authors emphasize CUDA randomness and employed various strategies to assess the impact of GPU execution-related randomness. Our objectives align with those of [10] and our study employs more recent techniques to achieve

fully deterministic results. Furthermore, we investigate the sensitivity of the output with respect to different optimizers and random seeds across multiple domains. Scardapane et al. [11] provide a comprehensive overview on randomness in deep learning, detailing the complexities and applications of randomness. In a broader context, Dirnagl [12] considered the problem of reproducing any scientific work and investigated this across multiple domains, emphasizing the multifaceted nature of this problem. Pham et al. [2] studied the variance of performance of deep learning systems. Their results show substantial performance variance and a considerable knowledge gap among researchers about these inconsistencies. Chou et al. [13] promoted deterministic execution on GPU platforms, citing its benefits for reproducibility. Later, a benchmark study by Zhuang et al. [4] presented tooling insights to manage randomness, focusing on the interplay between algorithmic-level factors and implementation-level factors. They state that deterministic training can introduce significant overhead.

### III. METHODOLOGY

For our empirical reproducibility investigation, we consider various hyperparameter configurations across different domains, conducting one fully deterministic and multiple randomized training runs. For the latter, we tightly control all sources of randomness besides CUDA-induced randomness caused by non-deterministic implementations of certain operations.

To mitigate randomness in deep learning applications, we fix seeds to five different random values. This practice, while limiting randomness up to a certain point, ensures more consistent results for random operations such as weight initialization, data shuffling, and data augmentation [14]. To investigate the role of optimizers, we use the two widely used optimizers ADAM [15] and SGD with momentum [16]. We then study the sensitivity of these different configurations to CUDA-induced randomness. An overview of the setup is shown in Fig. 1.

As depicted in Fig. 1, CUDA provides two settings: non-deterministic and deterministic. We conducted experiments on three datasets: CIFAR-10 [17], SDNET2018 [18], and CBIS-DDSM [19], with 20, 15, and 10 runs respectively. Each run was performed using fixed seed configurations under nondeterministic CUDA settings. Additionally, each fixed seed configuration was also tested once under fully deterministic settings. Consistency in the experimental framework was ensured by maintaining the same libraries, their versions, hardware, and other environmental factors that could affect randomness. Furthermore, the influence of two commonly used optimizers on the outcomes was evaluated. Overall, we evaluated a total of 480 experimental runs across the three datasets.

CIFAR-10 [17] is a standard computer vision dataset with 60,000 color images across 10 classes. SDNET2018 [18] is a real-world dataset with 56,000 labeled images for concrete crack detection. CBIS-DDSM [20] is another real-world dataset from a different domain, featuring around 10,000 mammography images categorized into benign and malignant

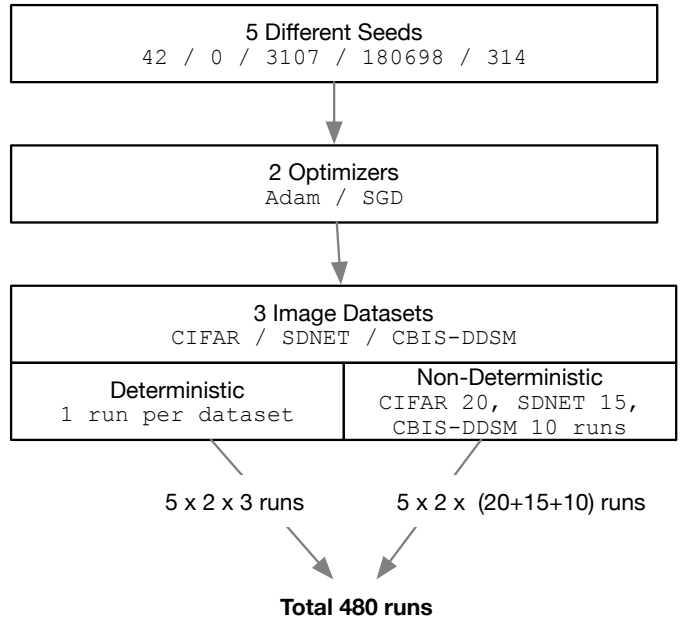


Fig. 1: Experimentation setup. 20, 15 and 10 runs for CIFAR, SDNET and CBIS-DDSM, respectively per seed and optimizer in the non-deterministic setup, 480 runs in total.

cases. We selected those datasets based on availability, citation frequency, and relevance to our research.

For model architectures, we employ ResNet [21], PreActResNet [22], and MobileNet [23] for image classification tasks due to their effectiveness and community recognition. ResNet tackles training challenges in deep networks with “residual blocks”, while PreActResNet optimizes performance through pre-activation integration. MobileNet, designed for resource-constrained devices, ensures efficiency without performance compromise. These choices were made considering efficacy, ease of implementation, and alignment with our research objectives.

All experiments were executed on a High-Performance Computer (HPC) infrastructure at the Institute for AI in Medicine [24] using SLURM [25], with monitoring facilitated by Weights & Biases (W&B) [26].

### IV. RESULTS

Table I summarizes the worst and best performance metrics out of a total of 480 runs obtained across the three tasks at hand. The numbers show the impact of both the random seed and CUDA related randomness. We evaluated the performance of different configurations on three distinct applications: classical CIFAR-10 benchmark, concrete crack detection with the SDNET2018 dataset, and medical imaging with the CBIS-DDSM dataset.

Our results for CIFAR-10 align with [27], with Stochastic Gradient Descent (SGD) [16] converging to more similar accuracies than Adaptive Moment Estimation (ADAM) [15]. Our results are also consistent with [22], even though our approach utilized a simpler network architecture.

TABLE I: Aggregated optimizer performance metrics for every run each task with maximum and minimum values with respective evaluation method.

| Dataset   | Metric | ADAM (%) |       | SGD (%) |       |
|-----------|--------|----------|-------|---------|-------|
|           |        | Max      | Min   | Max     | Min   |
| CIFAR-10  | Acc.   | 93.57    | 91.11 | 95.12   | 94.41 |
| SDNET2018 | F1     | 94.20    | 93.33 | 93.52   | 91.95 |
| CBIS-DDSM | AUC    | 80.49    | 76.88 | 79.35   | 73.73 |

For concrete crack detection, we report F1-score, as performance differences between optimizers were more pronounced. In the concrete crack detection case, our methodology shows improvement over the foundational work by [28], indicating the effectiveness of the chosen model in real-world scenarios.

For the medical imaging analysis using the CBIS-DDSM dataset, we report AUC [29] scores, a critical metric in this domain. Our findings align with those presented in the work of [30], albeit without employing GMIC (Globally-aware Multiple Instance Classifier) [31], which is known for its low-memory consumption while enabling higher resolution.

Table II shows detailed results from all configurations, highlighting the variability in performance that can occur if CUDA randomness is not controlled. In particular, in the CBSI-DDSM task, a clear gap of a maximum difference of 4.77% between the deterministic and non-deterministic runs with a random seed of 3407 and the SGD optimizer is noticeable.

#### Performance Variance and Tradeoffs

Our study employs distinct pipelines and metrics for each task, making direct performance comparisons across tasks challenging. However, by analyzing variances, we can assess task sensitivities to inherent randomness across the three distinct tasks. Additionally, for each seed and optimizer configuration, we have one fully deterministic configuration. By comparing the means of the non-deterministic runs with that particular fully deterministic run, we can get insights about the implications of CUDA randomness in terms of runtime and performance.

In analyzing the CBIS-DDSM task, as summarized in Table III, it is evident that the variability in performance metrics across different seeds and optimizers is noteworthy. For both, the SGD and the ADAM optimizer, we observe fluctuations in AUC scores, that are more pronounced in the ADAM optimizer. In particular, the ADAM optimizer at seed 0 shows the largest standard deviation in F1-score overall. The impact of deterministic execution on performance varied, with decreases of up to 2% for seed 314 and increases of up to 1.4% for seed 0. Such findings highlight the stochastic nature of model training outcomes in relation to seed selection and optimizer choice. Additionally, we infer from Table IV that runtime trade-offs from deterministic execution are generally small (once even in favor of the deterministic run) and at most incur a 16% longer runtime.

TABLE II: Comparison of non-deterministic means ( $\overline{ND}$ ) and deterministic (D) runs for CIFAR-10, SDNET, and CBIS-DDSM datasets across various configurations. The results show the performance metrics (Accuracy for CIFAR-10, F1-Score for SDNET, and AUC for CBIS-DDSM) with their respective configurations and the percentage change ( $\Delta\%$ ). The max difference (in %) for each configuration is shown as well ( $\Delta S$ ).

| Dataset                | Configuration          | $\overline{ND}$ | D     | $\Delta\%$ | $\Delta S(\%)$ |
|------------------------|------------------------|-----------------|-------|------------|----------------|
| CIFAR-10<br>(Accuracy) | ADAM <sub>0</sub>      | 92.57           | 92.19 | 0.419      | 0.92           |
|                        | SGD <sub>0</sub>       | 94.80           | 94.96 | -0.156     | 0.52           |
|                        | ADAM <sub>180698</sub> | 93.07           | 92.22 | 0.924      | 0.89           |
|                        | SGD <sub>180698</sub>  | 94.78           | 94.93 | 0.158      | 0.49           |
|                        | ADAM <sub>314</sub>    | 92.15           | 92.17 | -0.016     | 1.80           |
|                        | SGD <sub>314</sub>     | 94.80           | 94.71 | 0.097      | 0.5            |
|                        | ADAM <sub>3407</sub>   | 92.51           | 92.72 | -0.210     | 1.81           |
|                        | SGD <sub>3407</sub>    | 94.66           | 94.59 | 0.083      | 0.42           |
|                        | ADAM <sub>42</sub>     | 92.57           | 92.71 | -0.143     | 1.62           |
|                        | SGD <sub>42</sub>      | 94.76           | 94.81 | -0.048     | 0.69           |
| SDNET<br>(F1-Score)    | ADAM <sub>0</sub>      | 93.26           | 93.70 | -0.465     | 0.30           |
|                        | SGD <sub>0</sub>       | 92.34           | 92.64 | -0.322     | 0.98           |
|                        | ADAM <sub>180698</sub> | 93.45           | 93.82 | -0.386     | 0.41           |
|                        | SGD <sub>180698</sub>  | 92.24           | 92.12 | 0.138      | 0.37           |
|                        | ADAM <sub>314</sub>    | 93.17           | 93.14 | 0.033      | 0.45           |
|                        | SGD <sub>314</sub>     | 92.29           | 91.58 | 0.787      | 0.64           |
|                        | ADAM <sub>3407</sub>   | 93.35           | 93.29 | 0.070      | 0.21           |
|                        | SGD <sub>3407</sub>    | 91.50           | 92.03 | -0.571     | 1.19           |
|                        | ADAM <sub>42</sub>     | 93.30           | 93.37 | 0.066      | 0.66           |
|                        | SGD <sub>42</sub>      | 92.51           | 92.31 | 0.214      | 0.26           |
| CBIS-DDSM<br>(AUC)     | ADAM <sub>0</sub>      | 79.26           | 78.17 | 1.399      | 1.00           |
|                        | SGD <sub>0</sub>       | 76.69           | 77.35 | -0.854     | 3.86           |
|                        | ADAM <sub>180698</sub> | 78.14           | 77.16 | 1.266      | 1.92           |
|                        | SGD <sub>180698</sub>  | 76.42           | 77.73 | -1.681     | 2.81           |
|                        | ADAM <sub>314</sub>    | 77.75           | 79.36 | -2.022     | 3.22           |
|                        | SGD <sub>314</sub>     | 77.18           | 77.70 | -0.674     | 4.40           |
|                        | ADAM <sub>3407</sub>   | 79.69           | 78.77 | 1.172      | 2.46           |
|                        | SGD <sub>3407</sub>    | 77.23           | 76.56 | 0.876      | 4.77           |
|                        | ADAM <sub>42</sub>     | 78.38           | 79.65 | -1.596     | 2.13           |
|                        | SGD <sub>42</sub>      | 77.24           | 76.95 | 0.364      | 2.23           |

#### T-Test with One-Sample Mean

To evaluate if non-deterministic run performances significantly diverge from deterministic runs, we employed a t-test, leveraging the consistency of deterministic runs as the population mean. This approach is premised on the repeatability of deterministic runs, which are posited to accurately represent the "true" population mean. The hypotheses are succinctly framed as:  $H_0$  (**Null**): There is no significant difference between deterministic and non-deterministic runs, indicating the effect of CUDA randomness cannot be conclusively determined.  $H_1$  (**Alternative**): A significant difference suggests CUDA randomness does influence results, leading to the rejection of  $H_0$ . This methodology enables a direct assessment of CUDA randomness' impact on performance metrics.

The analysis of one-sample t-test results, as summarized in Table V, indicates that CUDA randomness affects the performance outcomes across the CIFAR-10, CBIS-DDSM, and SDNET datasets. For the CIFAR-10 dataset, statistically significant differences were observed in 50% of the config-

TABLE III: Deterministic and non-deterministic performance comparison for the CBIS-DDSM dataset with two optimizers, ADAM and SGD, expressed in AUC score. The first column lists all the seed configurations.  $AUC_{det}$  represents the deterministic run for each seed configuration.  $AUC_{n-det}$  represents the mean of non-deterministic runs for each seed configuration.  $\Delta\%$  indicates the performance difference in percentage between the deterministic and non-deterministic runs.  $\sigma_{n-det(AUC)}$  shows the standard deviation of all runs for the respective seed configuration with AUC scores, and  $\sigma_{n-det(F1)}$  presents it for the F1-score.

| Seed   | ADAM        |               |            |                       |                      | SGD         |               |            |                       |                      |
|--------|-------------|---------------|------------|-----------------------|----------------------|-------------|---------------|------------|-----------------------|----------------------|
|        | $AUC_{det}$ | $AUC_{n-det}$ | $\Delta\%$ | $\sigma_{n-det(AUC)}$ | $\sigma_{n-det(F1)}$ | $AUC_{det}$ | $AUC_{n-det}$ | $\Delta\%$ | $\sigma_{n-det(AUC)}$ | $\sigma_{n-det(F1)}$ |
| 0      | 0.7817      | 0.7903        | 1.11       | 0.0037                | 0.0498               | 0.7735      | 0.7664        | -0.93      | 0.0141                | 0.0228               |
| 180698 | 0.7716      | 0.7796        | 1.03       | 0.0057                | 0.0222               | 0.7773      | 0.7649        | -1.60      | 0.0090                | 0.0248               |
| 314    | 0.7936      | 0.7835        | -1.27      | 0.0093                | 0.0302               | 0.7770      | 0.7737        | -0.44      | 0.0158                | 0.0197               |
| 3407   | 0.7877      | 0.7940        | 0.80       | 0.0086                | 0.0244               | 0.7656      | 0.7698        | 0.54       | 0.0142                | 0.0190               |
| 42     | 0.7965      | 0.7829        | -1.71      | 0.0066                | 0.0262               | 0.7695      | 0.7731        | 0.46       | 0.0082                | 0.0185               |

TABLE IV: Deterministic and non-deterministic runtime comparison for the CBIS-DDSM dataset with two optimizers, ADAM and SGD, expressed in minutes. The first column lists all the seed configurations.  $\mu_{det}$  represents the deterministic runtime for each seed configuration.  $\mu_{n-det}$  represents the mean non-deterministic runtime for each seed configuration.  $\Delta\%$  indicates the runtime difference in percentage between the deterministic and non-deterministic runs.

| Config | Optimizer | $\mu_{det}$ (min) | $\mu_{n-det}$ (min) | $\Delta\%$ |
|--------|-----------|-------------------|---------------------|------------|
| 0      | ADAM      | 343.63            | 319.85              | -6.92      |
|        | SGD       | 398.45            | 358.88              | -9.93      |
| 180698 | ADAM      | 423.07            | 409.54              | -3.20      |
|        | SGD       | 399.05            | 393.92              | -1.29      |
| 314    | ADAM      | 407.55            | 370.17              | -9.17      |
|        | SGD       | 369.20            | 367.45              | -0.47      |
| 3407   | ADAM      | 414.48            | 382.11              | -7.81      |
|        | SGD       | 364.17            | 303.99              | -16.53     |
| 42     | ADAM      | 360.46            | 355.44              | -1.39      |
|        | SGD       | 366.48            | 376.31              | 2.68       |

urations, with ADAM showing a higher average deviation (0.517% for significant runs, 0.3484% overall) compared to SGD (0.1465% for significant runs, 0.1042% overall). In the CBIS-DDSM dataset, all ADAM configurations were significant, highlighting its sensitivity, whereas only one SGD configuration showed statistical significance, with average deviations of 1.68% for significant runs and 0.889% overall for SGD, and 1.491% for both significant and overall runs for ADAM. The SDNET dataset showed a balance of significant outcomes among configurations for both optimizers, with ADAM’s deviations at 0.425% for significant runs and 0.204% overall, versus SGD’s 0.441% for significant runs and 0.406% overall. These findings underscore ADAM’s higher sensitivity to CUDA randomness compared to SGD, reflected in the greater number of significant configurations and larger deviation percentages.

TABLE V: Number of significant configurations ( $p \leq 0.05$ , as determined by a t-test) from each dataset with respect to the optimizers, and average differences in performance between the significant configurations and all configurations.

|                  | Sig. Confgs | Avg (Sig.) | Avg (All) |
|------------------|-------------|------------|-----------|
| <b>CIFAR-10</b>  |             |            |           |
| SGD              | 2/5         | 0.1465%    | 0.1042%   |
| ADAM             | 3/5         | 0.517%     | 0.3484%   |
| <b>CBIS-DDSM</b> |             |            |           |
| SGD              | 1/5         | 1.68%      | 0.889%    |
| ADAM             | All         | 1.491%     | 1.491%    |
| <b>SDNET</b>     |             |            |           |
| SGD              | 3/5         | 0.441%     | 0.406%    |
| ADAM             | 2/5         | 0.425%     | 0.204%    |

#### Similarities of Model Weights

Figs. 2 and 3 show the similarities of embeddings across datasets and optimizers. The mean similarities provide a general overview, while minimum similarities show the extreme points of two runs affected by inherent CUDA execution randomness. The minimum similarity provides insight into the maximum potential impact of this randomness. In the figures, a value of 1 indicates that the embeddings were identical, whereas a value of 0 indicates that they were completely orthogonal.

Fig. 2 illustrates the last layer similarities for the ADAM optimizer across the three datasets. For the CIFAR-10 dataset, we observe the lowest similarity and largest variations. In later epochs, there seems to be a convergence of embedding representations as similarity values stabilize. In the CBIS-DDSM dataset, there is a consistent decline in similarity. This consistent reduction may be attributed to the effects of fine-tuning from ImageNet [32]-initialized weights rather than training from scratch. For the SDNET dataset, a pronounced initial drop is observed, indicating a swift divergence of weights. Yet, the similarities in subsequent epochs decline more gradually, hinting at a plateau in weight divergence.

Fig. 3 shows the embedding similarities for the SGD optimizer. Overall, we observe similar trends as for the ADAM op-

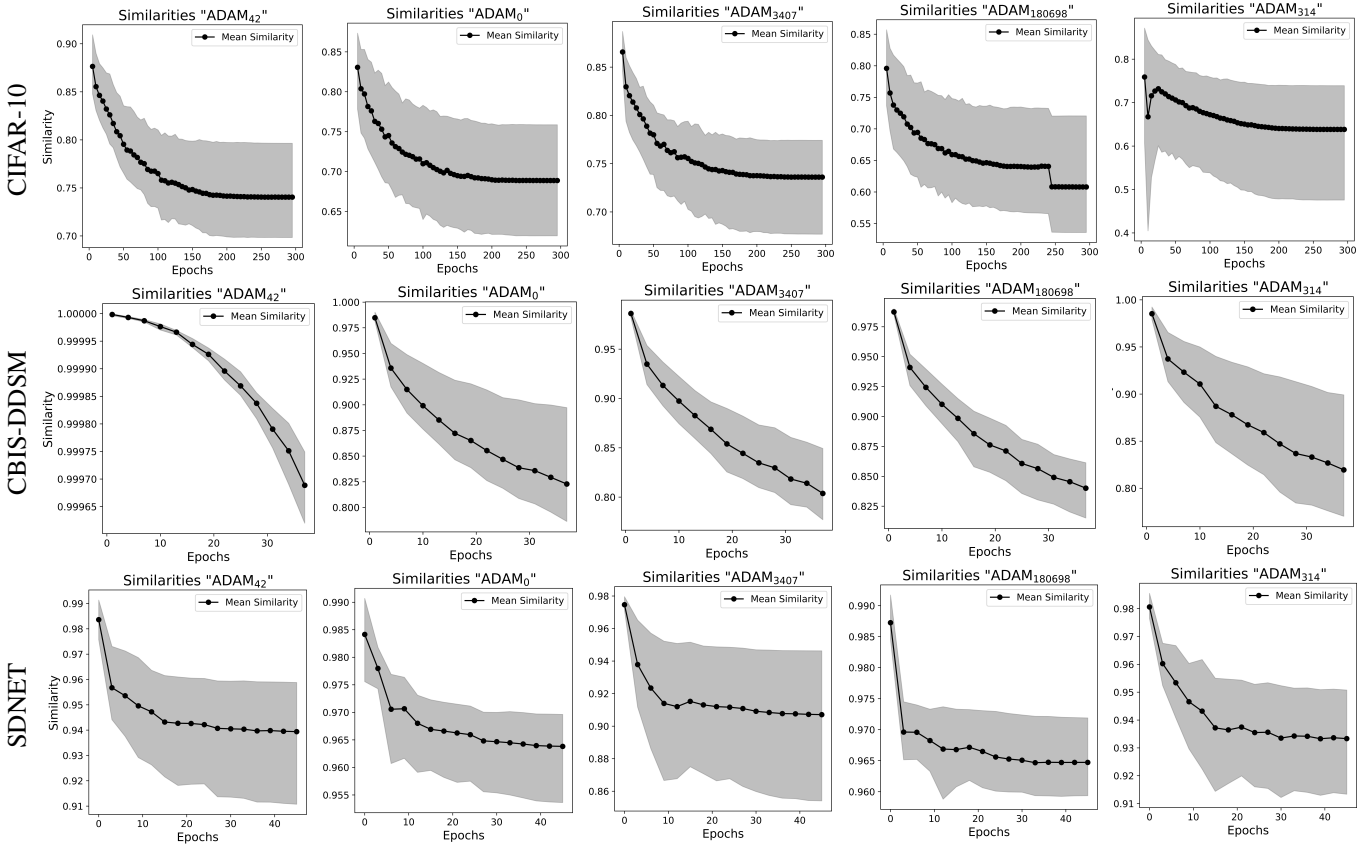


Fig. 2: Cosine similarity of embeddings in the last linear layer of the models with respect to epoch number. Showing max, min, and mean cosine similarity values with Adam optimizer for each dataset (rows) and seed (column).

timizer, but less pronounced differences in similarities. Again, CIFAR-10 has the lowest similarity and largest variation, but similarities are much higher as with the ADAM optimizer. For the CBIS-DDSM dataset, there is a constant decrease in similarity, but embedding differences are subtle. On the SDNET dataset, we again observe an initial drop, followed by a plateau. However, again, differences are subtle.

## V. ENVIRONMENTAL IMPACT OF THE EXPERIMENTS

In scientific research, it is crucial to consider not only the direct results of experiments but also the broader implications and consequences of the research process. While the following environmental assessment is not directly tied to our primary results, it represents an essential facet of our experiments. We believe it is our responsibility to report on the environmental footprint of our work, given the increasing global emphasis on sustainability and the environmental impact of computational practices. Furthermore, we posit that the environmental implications of computational experiments are becoming increasingly significant in the context of sustainable research practices. This perspective aligns with the findings of Ulmer et al. [33], emphasizing the importance of understanding and reporting the environmental consequences of experimental work.

Our experiments were conducted using HPC resources located in Essen, Germany. The region’s electricity generation has a carbon efficiency of 0.385 kgCO<sub>2</sub>eq/kWh [34], with approximately 43% [35] of the electricity being sourced from fossil fuels. To estimate the carbon footprint of our experiments, we utilized the Machine Learning Impact calculator, as presented by Lacoste et al. [36]. This calculator provides a comprehensive framework to quantify the carbon emissions associated with machine learning experiments, considering both the energy consumption of computational resources and the carbon efficiency of the electricity source.

From Table VI, it is evident that while the energy consumption and associated carbon emissions for the reported experiments (“Experiment runs”) might not be significant, the overall environmental impact is considerably higher when accounting for all computational activities, including tests, debugging, and experimental setups (“All runs”). This highlights the broader environmental cost of the entire research process, not just the final reported results. It underscores the importance of energy-efficient algorithms and practices in machine learning research, especially in regions heavily reliant on fossil fuels for electricity generation.

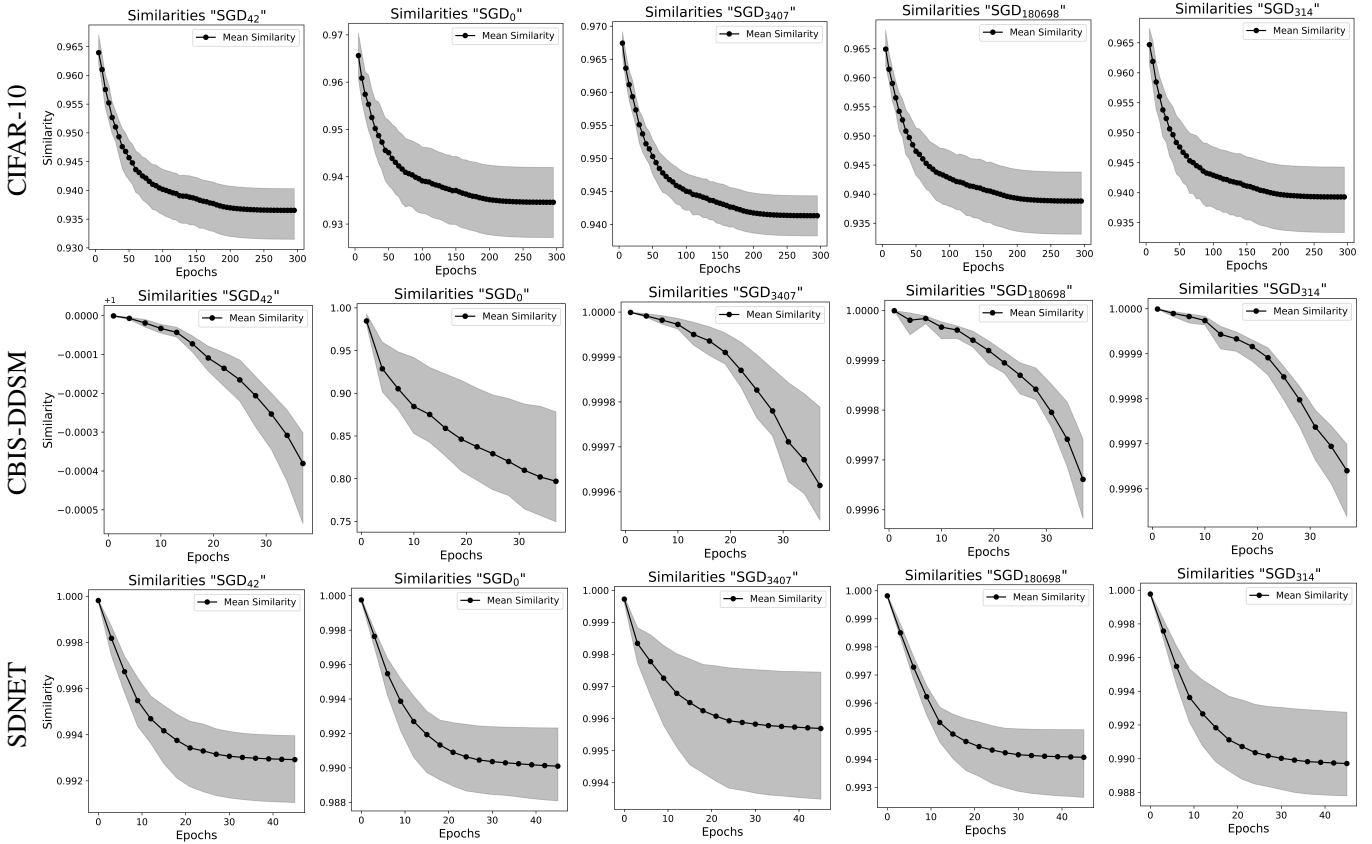


Fig. 3: Cosine similarity of embeddings in the last linear layer of the models with respect to epoch number. Showing max, min, and mean cosine similarity values with SGD optimizer for each dataset (rows) and seed (column).

TABLE VI: Energy consumption and carbon dioxide (CO<sub>2</sub>) emission for different tasks. The table shows the energy consumption in kilowatt-hours (kWh) and the corresponding CO<sub>2</sub> emissions in kilograms (kg) under two categories: Experiment runs and All runs. The SUM row provides the total energy consumption for each run type, and the CO<sub>2</sub> row calculates the emissions based on the formula CO<sub>2</sub> (kg) = Energy (kWh) × 0.385.

|                      | Experiment runs | All runs |
|----------------------|-----------------|----------|
| Cifar-10 (kWh)       | 69.89           | 117.37   |
| CBIS-DDSM (kWh)      | 116.04          | 134.594  |
| SDNET (kWh)          | 89.29           | 114.78   |
| SUM (kWh)            | 275.22          | 366.744  |
| CO <sub>2</sub> (kg) | 105.06          | 141.69   |

## VI. DISCUSSION AND CONCLUSION

From the analysis presented in Table III, it becomes clear that CUDA-randomness significantly influences performance variability, with the impact varying across three datasets and two optimizers. The choice of optimizer shows dependency on the specific dataset, indicating that the interplay between optimizer and dataset characteristics is crucial. Moreover, we

observe that different performance metrics exhibit varied levels of variability, suggesting that the choice of metric is pivotal in understanding the performance landscape. Additionally, variability introduced by different seed values is non-negligible, further complicating the performance analysis. Most notably, the mammography task demonstrates significantly greater performance variance compared to the other datasets, highlighting the task-specific nature of CUDA-randomness effects.

In examining the tradeoffs between deterministic and non-deterministic modes, our findings reveal nuanced differences in performance and runtime across various configurations (cf. Tables III and IV). While Zhuang et al. [4] and the PyTorch documentation<sup>1</sup> suggest that deterministic execution generally incurs higher runtime and lower performance, our experiments show this is not always the case. The performance differences between the two modes are usually within a 1% margin for CIFAR-10 and SDNET datasets, indicating that deterministic settings could be favored for reproducibility without significantly sacrificing performance. However, for the mammography task, the performance gap occasionally exceeds 1%, challenging the assumption that deterministic operations consistently yield higher performance or vice versa.

<sup>1</sup><https://pytorch.org/docs/stable/notes/randomness.html>  
 Accessed: 2023-10-09

Additionally, runtime analyses revealed that deterministic execution does not invariably lead to longer training times across all datasets. These findings emphasize the importance of considering specific dataset characteristics and algorithmic choices in PyTorch when evaluating the tradeoffs between deterministic and non-deterministic modes.

Our analysis of statistical significance in performance differences (cf. Table V) showed that in particular the real-world mammography task is heavily influenced by CUDA randomness. We not only observed significant differences in all runs of the ADAM optimizer, but also the largest deviation of up to 1.68% in all configurations that were significant (both for ADAM and SGD). This indicates that seed value selection can be crucial for the reproducibility of results in this task, and that the choice of optimizer may heavily influence the robustness of results.

To enhance reproducibility and robustness in deep learning research, we propose several strategies based on our study's insights. Firstly, adopting fully deterministic settings can offer significant benefits, as our results indicate, by zeroing variability and improving reproducibility. Conducting experiments across a range of seed values is also essential, allowing for a deeper understanding of how specific configurations impact outcomes. Moreover, ensuring full disclosure of all experimental settings, including configurations and software versions, is critical for enabling others to replicate and validate findings.

Due to time and hardware constraints, runs per configuration were limited. Future studies could enhance robustness and depth of understanding by increasing the number of experimental runs. Our selected datasets are representative of application areas, but are still limited in scope. Future research could explore larger or more diverse datasets, such as ImageNet and CIFAR-100, to assess reproducibility across different scales and types of data. The selection of hyperparameters, informed by existing literature, suggests that a more exhaustive search might reveal further insights into hyperparameter influence on randomness. This study's focus on CUDA-induced randomness identifies a gap in the literature, indicating the necessity for additional research on computational consistency within CUDA architecture. Moreover, exploring the impact of different neural network architectures and distributed deep learning settings on reproducibility could be a further area of investigation. Lastly, considering different computational frameworks beyond PyTorch, such as TensorFlow, could offer a broader perspective on reproducibility challenges.

In summary, we derived the following insights from our study.

**Variability might be due to random seeds and chosen optimizers.** Empirical evidence highlights that model performance and variance are influenced by different seed settings and optimizer selections. Evaluating models across a range of seed configurations is essential for identifying setups that not only achieve optimal performance but also maintain minimal variance. Though widely used, the ADAM optimizer showed comparably lower robustness against CUDA-induced randomness in our study.

**Determinism introduces minor computational overhead and might slightly decrease predictive performance.** Our results show that deterministic execution usually introduces a negligible computational overhead while it is advantageous for reproducibility. Nonetheless, determinism can enhance performance by up to 2% or result in reductions exceeding 1%. This performance variability necessitates a careful decision-making process regarding the use of deterministic versus non-deterministic execution, based on the specific goals and performance criteria of the model.

**The effect of randomness is domain-specific.** The influence of randomness during training exhibits significant variation across different domains, with the medical imaging domain, exemplified by the mammography dataset, being particularly susceptible to randomness. This variation accentuates the reproducibility challenges in medical imaging and emphasizes the importance of domain-specific approaches in model training and evaluation.

#### ACKNOWLEDGMENTS

We thank the doctoral researchers from the Research Training Group 2535 Knowledge- and Data-Based Personalization of Medicine at the Point of Care (WisPerMed), Hendrik Damm, Helmut Becker, Tabea Pakull, and Mikel Bahn, who reviewed this paper and provided valuable comments.

#### REFERENCES

- [1] S. Kapoor and A. Narayanan, "Leakage and the reproducibility crisis in machine-learning-based science," *Patterns*, vol. 4, no. 9, p. 100804, 2023. [Online]. Available: <https://www.sciencedirect.com/science/article/pii/S2666389923001599>
- [2] H. V. Pham, S. Qian, J. Wang, T. Lutellier, J. Rosenthal, L. Tan, Y. Yu, and N. Nagappan, "Problems and opportunities in training deep learning software systems: An analysis of variance," in *Proceedings of the 35th IEEE/ACM International Conference on Automated Software Engineering*, 2020, pp. 771–783.
- [3] S. Piramuthu, M. J. Shaw, and J. A. Gentry, "A classification approach using multi-layered neural networks," *Decision Support Systems*, vol. 11, no. 5, pp. 509–525, 1994. [Online]. Available: <https://www.sciencedirect.com/science/article/pii/0167923694900221>
- [4] D. Zhuang, X. Zhang, S. Song, and S. Hooker, "Randomness in neural network training: Characterizing the impact of tooling," *Proceedings of Machine Learning and Systems*, vol. 4, pp. 316–336, 2022.
- [5] R. R. Snapp and G. I. Shamir, "Synthesizing irreproducibility in deep networks," *arXiv preprint arXiv:2102.10696*, 2021.
- [6] W. Jeon, G. Ko, J. Lee, H. Lee, D. Ha, and W. W. Ro, "Chapter six - deep learning with gpus," in *Hardware Accelerator Systems for Artificial Intelligence and Machine Learning*, ser. Advances in Computers, S. Kim and G. C. Deka, Eds. Elsevier, 2021, vol. 122, pp. 167–215. [Online]. Available: <https://www.sciencedirect.com/science/article/pii/S0065245820300905>
- [7] S. Hooker, "The hardware lottery," *Communications of the ACM*, vol. 64, no. 12, pp. 58–65, 2021.
- [8] S. N. Goodman, D. Fanelli, and J. P. A. Ioannidis, "What does research reproducibility mean?" *Science Translational Medicine*, vol. 8, no. 341, pp. 341ps12–341ps12, 2016.
- [9] S. Raste, R. Singh, J. Vaughan, and V. N. Nair, "Quantifying inherent randomness in machine learning algorithms," 2022. [Online]. Available: <https://arxiv.org/abs/2206.12353>
- [10] B. Chen, M. Wen, Y. Shi, D. Lin, G. K. Rajbahadur, and Z. M. J. Jiang, "Towards training reproducible deep learning models," in *Proceedings of the 44th International Conference on Software Engineering*, ser. ICSE '22. New York, NY, USA: Association for Computing Machinery, 2022, p. 2202–2214. [Online]. Available: <https://doi.org/10.1145/3510003.3510163>

- [11] S. Scardapane and D. Wang, “Randomness in neural networks: an overview,” *Wiley Interdisciplinary Reviews: Data Mining and Knowledge Discovery*, vol. 7, no. 2, p. e1200, 2017.
- [12] U. Dirnagl, “Rethinking research reproducibility,” *The EMBO Journal*, vol. 38, no. 2, p. e101117, 2019.
- [13] Y. H. Chou, C. Ng, S. Cattell, J. Intan, M. D. Sinclair, J. Devietti, T. G. Rogers, and T. M. Aamodt, “Deterministic atomic buffering,” in *2020 53rd Annual IEEE/ACM International Symposium on Microarchitecture (MICRO)*. IEEE, 2020, pp. 981–995.
- [14] Y. Ji, D. Kaestner, O. Wirth, and C. Wressnegger, “Randomness is the root of all evil: More reliable evaluation of deep active learning,” in *Proceedings of the IEEE/CVF Winter Conference on Applications of Computer Vision (WACV)*, January 2023, pp. 3943–3952.
- [15] Z. Zhang, “Improved adam optimizer for deep neural networks,” in *2018 IEEE/ACM 26th International Symposium on Quality of Service (IWQoS)*, 2018, pp. 1–2.
- [16] Y. Liu, Y. Gao, and W. Yin, “An improved analysis of stochastic gradient descent with momentum,” in *Advances in Neural Information Processing Systems*, H. Larochelle, M. Ranzato, R. Hadsell, M. Balcan, and H. Lin, Eds., vol. 33. Curran Associates, Inc., 2020, pp. 18261–18271. [Online]. Available: [https://proceedings.neurips.cc/paper\\_files/paper/2020/file/d3f5d4de09ea19461dab00590df91e4f-Paper.pdf](https://proceedings.neurips.cc/paper_files/paper/2020/file/d3f5d4de09ea19461dab00590df91e4f-Paper.pdf)
- [17] A. Krizhevsky, “Learning multiple layers of features from tiny images,” *h*, pp. 32–33, 2009. [Online]. Available: <https://www.cs.toronto.edu/~kriz/learning-features-2009-TR.pdf>
- [18] M. Maguire, S. Dorafshan, and R. J. Thomas, “Sdnet2018: A concrete crack image dataset for machine learning applications,” *hr*, 2018.
- [19] F. A. Spanhol, L. S. Oliveira, C. Petitjean, and L. Heutte, “A dataset for breast cancer histopathological image classification,” *Ieee transactions on biomedical engineering*, vol. 63, no. 7, pp. 1455–1462, 2015.
- [20] R. Sawyer-Lee, F. Gimenez, A. Hoogi, and D. Rubin, “Curated breast imaging subset of digital database for screening mammography (cbis-ddsm) (version 1) [data set],” 2016, accessed: 28/04/2022. [Online]. Available: <https://doi.org/10.7937/K9/TCIA.2016.7002S9CY>
- [21] K. He, X. Zhang, S. Ren, and J. Sun, “Deep residual learning for image recognition,” in *2016 IEEE Conference on Computer Vision and Pattern Recognition (CVPR)*, 2016, pp. 770–778.
- [22] ———, “Identity mappings in deep residual networks,” in *Computer Vision - ECCV 2016*, B. Leibe, J. Matas, N. Sebe, and M. Welling, Eds. Cham: Springer International Publishing, 2016, pp. 630–645.
- [23] A. G. Howard, M. Zhu, B. Chen, D. Kalenichenko, W. Wang, T. Weyand, M. Andreetto, and H. Adam, “Mobilenets: Efficient convolutional neural networks for mobile vision applications,” *CoRR*, vol. abs/1704.04861, 2017. [Online]. Available: <http://arxiv.org/abs/1704.04861>
- [24] H. F. Schmidt, J. Schlötterer, M. Bargull, E. Nasca, R. Aydelott, C. Seifert, and F. Meyer, “Towards a trustworthy, secure and reliable enclave for machine learning in a hospital setting: The Essen Medical Computing Platform (EMCP),” in *IEEE International Conference on Cognitive Machine Intelligence (CogMI)*, 2021, pp. 116–123.
- [25] A. B. Yoo, M. A. Jette, and M. Grondona, “Slurm: Simple linux utility for resource management,” in *Workshop on job scheduling strategies for parallel processing*. Springer, 2003, pp. 44–60.
- [26] L. Biewald, “Experiment tracking with weights and biases,” 2020, software available from wandb.com. [Online]. Available: <https://www.wandb.com/>
- [27] A. Gupta, R. Ramanath, J. Shi, and S. S. Keerthi, “Adam vs. sgd: Closing the generalization gap on image classification,” in *OPT2021: 13th Annual Workshop on Optimization for Machine Learning*, 2021.
- [28] S. Dorafshan, R. J. Thomas, and M. Maguire, “Sdnet2018: An annotated image dataset for non-contact concrete crack detection using deep convolutional neural networks,” *Data in brief*, vol. 21, pp. 1664–1668, 2018.
- [29] A. P. Bradley, “The use of the area under the roc curve in the evaluation of machine learning algorithms,” *Pattern recognition*, vol. 30, no. 7, pp. 1145–1159, 1997.
- [30] Y. Shen, N. Wu, J. Phang, J. Park, K. Liu, S. Tyagi, L. Heacock, S. G. Kim, L. Moy, K. Cho, and K. J. Geras, “An interpretable classifier for high-resolution breast cancer screening images utilizing weakly supervised localization,” *CoRR*, vol. abs/2002.07613, 2020. [Online]. Available: <https://arxiv.org/abs/2002.07613>
- [31] Y. Shen, N. Wu, J. Phang, J. Park, G. Kim, L. Moy, K. Cho, and K. J. Geras, “Globally-aware multiple instance classifier for breast cancer screening,” in *Machine Learning in Medical Imaging: 10th International Workshop, MLMI 2019, Held in Conjunction with MICCAI 2019, Shenzhen, China, October 13, 2019, Proceedings 10*. Springer, 2019, pp. 18–26.
- [32] J. Deng, W. Dong, R. Socher, L.-J. Li, K. Li, and L. Fei-Fei, “Imagenet: A large-scale hierarchical image database,” in *2009 IEEE Conference on Computer Vision and Pattern Recognition*, 2009, pp. 248–255.
- [33] D. Ulmer, E. Bassignana, M. Müller-Eberstein, D. Varab, M. Zhang, R. van der Goot, C. Hardmeier, and B. Plank, “Experimental standards for deep learning in natural language processing research,” in *Findings of the Association for Computational Linguistics: EMNLP 2022*. Abu Dhabi, United Arab Emirates: Association for Computational Linguistics, Dec. 2022, pp. 2673–2692. [Online]. Available: <https://aclanthology.org/2022.findings-emnlp.196>
- [34] O. W. in Data. (2023) Carbon intensity of electricity. Accessed: 2023-10-4. [Online]. Available: <https://ourworldindata.org/grapher/carbon-intensity-electricity>
- [35] Statista. (2022) Power mix in germany 2022. Accessed: October 7, 2024. [Online]. Available: <https://www.statista.com/statistics/736640/energy-mix-germany/>
- [36] A. Lacoste, A. Luccioni, V. Schmidt, and T. Dandres, “Quantifying the carbon emissions of machine learning,” *CoRR*, vol. abs/1910.09700, 2019. [Online]. Available: <http://arxiv.org/abs/1910.09700>

## APPENDIX

### A. Reproducing the Results

The datasets utilized in this study are publicly accessible. Details are as follows:

- CIFAR-10 Dataset: The dataset can be accessed from the University of Toronto’s website.<sup>2</sup>
- SDNET2018 Dataset: It is available on the Utah State University’s digital commons page.<sup>3</sup>
- CBIS-DDSM Dataset: The dataset is hosted on the Cancer Imaging Archive wiki.<sup>4</sup>

The codebase supporting this study is also open-source. The current GitHub repository is as follows:

<https://github.com/aix-group/repincv.git>

Within the repository, the code structure is organized into specific tasks:

- task1: CIFAR-10 experiments.
- task2(SDNET 2018): Concrete Crack Detection experiments.
- task3(CBIS-DDSM): Breast Cancer Imaging experiments.

Always refer to the official repository as it can get fixes or updates in the future.

*Instructions to Reproduce the Results:* While the CIFAR-10 and SDNET2018 datasets are set to auto-download if absent in the input directory, the CBIS-DDSM requires manual downloading due to its voluminous size. Once obtained, it should be relocated to the input directory. Subsequent image preprocessing steps are documented within the aforementioned repository.

<sup>2</sup><https://www.cs.toronto.edu/~kriz/cifar.html>, last accessed 15 November 2023

<sup>3</sup>[https://digitalcommons.usu.edu/all\\_datasets/48/](https://digitalcommons.usu.edu/all_datasets/48/), last accessed 22 October 2023

<sup>4</sup><https://wiki.cancerimagingarchive.net/pages/viewpage.action?pageId=22516629>, last accessed 10 December 2023



For the experimental sections of this study, the (W&B) platform was employed for result tracking. To replicate the findings, adhere to the following procedure:

*Securing the (W&B) API Key:*

- Initiate by visiting the Weights & Biases official site.
- Proceed to sign in or establish an account if not already registered.
- Access your personal settings to retrieve your unique API key.
- Copy the API key for upcoming phases.

For a guide on securing the (W&B) API key, consult the platform’s official documentation.<sup>5</sup>

Setup Instructions:

```
git clone https://github.com/mcml-group/
  repincv.git
cd repincv

wandb login

conda create --name repincv_env python=3.8
conda activate repincv_env

pip install -r requirements.txt

python run_experiments.py --task <task_name>
```

First, clone the repository and navigate into it. Next, log in to WandB; when prompted, paste the API key you obtained in the previous step. Then, create a new Conda environment named `repincv_env` with Python 3.8 and activate it. Install the necessary packages using the `requirements.txt` file, which is located in the root directory of the repository and contains the versions of the important packages used in the experiments. Finally, run the experiment script with `python run_experiments.py --task <task_name>`, replacing `<task_name>` with one of the following: `task1`, `task2`, or `task3`.

The cumulative training duration for all experiments was approximately 900 hours, equivalent to nearly five weeks of continuous computation on a single NVIDIA RTX A6000 GPU.

### B. Additional Tables and Graphs from the Experiment Data

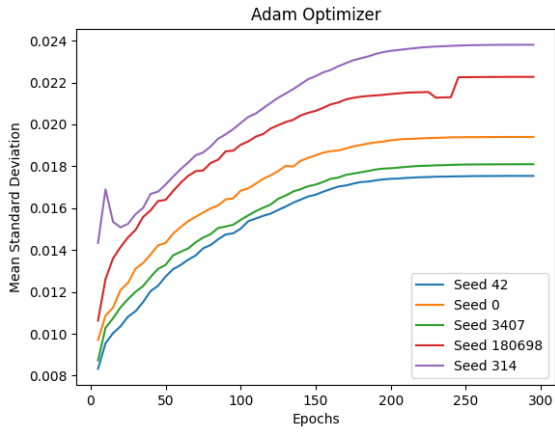
TABLE VII: Deterministic and non-deterministic runtime comparison for the CIFAR dataset with two optimizers, ADAM and SGD, expressed in minutes. The first column lists all the seed configurations.  $\bar{A}_{ND}$  represents the non-deterministic mean accuracy for each seed configuration.  $\bar{A}_D$  represents the deterministic accuracy for each seed configuration.  $\sigma$  indicates the runtime variation.  $\mu$  represents the mean runtime for deterministic and non-deterministic scenarios.

| Config | Optimizer | $\bar{A}_{ND}$ | $\bar{A}_D$ | $\sigma$ | $\mu_{ND}$ (min) | $\mu_D$ (min) |
|--------|-----------|----------------|-------------|----------|------------------|---------------|
| 0      | ADAM      | 0.925          | 0.922       | 0.0018   | 110.94           | 135.82        |
|        | SGD       | 0.948          | 0.950       | 0.0027   | 105.27           | 137.18        |
| 180698 | ADAM      | 0.930          | 0.922       | 0.0015   | 114.51           | 133.93        |
|        | SGD       | 0.947          | 0.949       | 0.0016   | 105.44           | 135.97        |
| 314    | ADAM      | 0.923          | 0.922       | 0.0009   | 115.74           | 133.48        |
|        | SGD       | 0.948          | 0.947       | 0.0043   | 103.90           | 134.58        |
| 3407   | ADAM      | 0.924          | 0.927       | 0.0010   | 114.07           | 135.18        |
|        | SGD       | 0.947          | 0.946       | 0.0035   | 106.69           | 132.38        |
| 42     | ADAM      | 0.925          | 0.927       | 0.0030   | 112.38           | 135.30        |
|        | SGD       | 0.947          | 0.948       | 0.0009   | 110.25           | 135.55        |

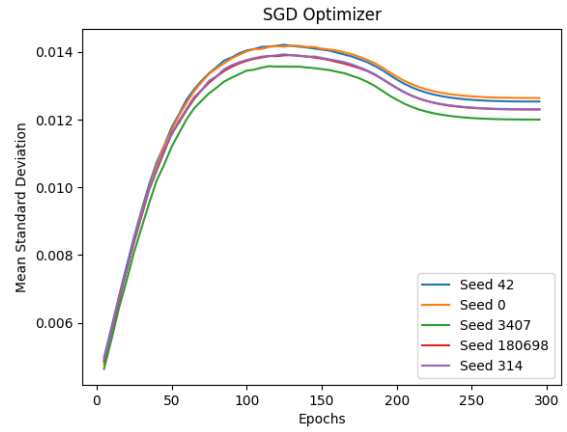
TABLE VIII: Deterministic and non-deterministic runtime comparison for the SDNET dataset with two optimizers, ADAM and SGD, expressed in minutes. The first column lists all the seed configurations.  $\bar{F1}_{ND}$  represents the non-deterministic mean F1 Score for each seed configuration.  $\bar{F1}_D$  represents the deterministic F1 Score for each seed configuration.  $\sigma$  indicates the runtime variation.  $\mu$  represents the mean runtime for deterministic and non-deterministic scenarios.

| Config | Optimizer | $\bar{F1}_{ND}$ | $\bar{F1}_D$ | $\sigma$ | $\mu_{ND}$ (min) | $\mu_D$ (min) |
|--------|-----------|-----------------|--------------|----------|------------------|---------------|
| 314    | ADAM      | 0.938           | 0.935        | 0.0018   | 166.63           | 153.20        |
|        | SGD       | 0.929           | 0.922        | 0.0027   | 179.06           | 203.12        |
| 180698 | ADAM      | 0.940           | 0.939        | 0.0015   | 170.97           | 157.40        |
|        | SGD       | 0.930           | 0.929        | 0.0016   | 164.38           | 159.08        |
| 3407   | ADAM      | 0.939           | 0.937        | 0.0009   | 176.83           | 213.62        |
|        | SGD       | 0.926           | 0.928        | 0.0043   | 164.97           | 150.08        |
| 0      | ADAM      | 0.939           | 0.939        | 0.0010   | 161.15           | 161.33        |
|        | SGD       | 0.930           | 0.928        | 0.0035   | 210.25           | 221.62        |
| 42     | ADAM      | 0.936           | 0.941        | 0.0030   | 165.09           | 170.87        |
|        | SGD       | 0.931           | 0.931        | 0.0009   | 157.04           | 152.25        |

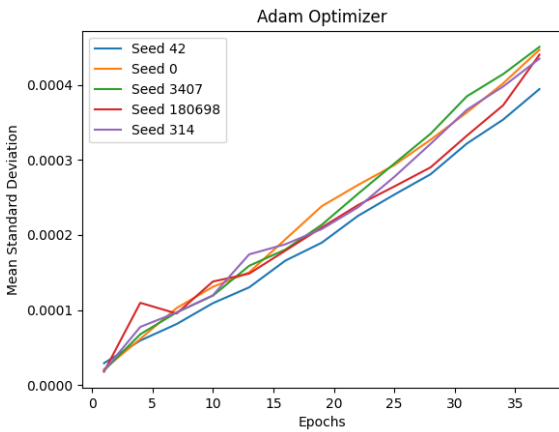
<sup>5</sup><https://docs.wandb.ai/quickstart>



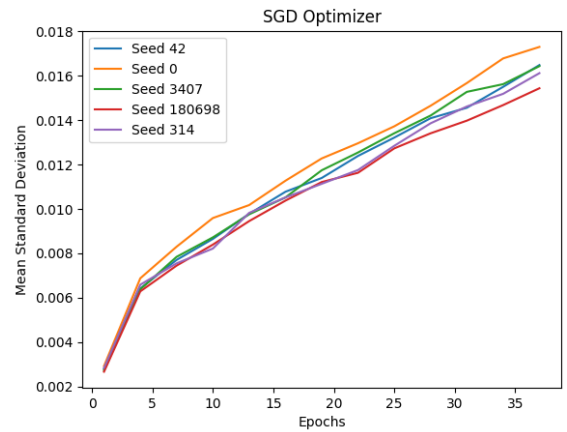
(a) CIFAR-10 Variances for ADAM Optimizer



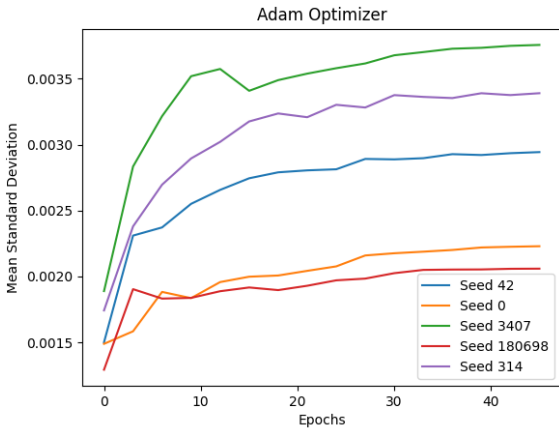
(b) CIFAR-10 Variances for SGD Optimizer



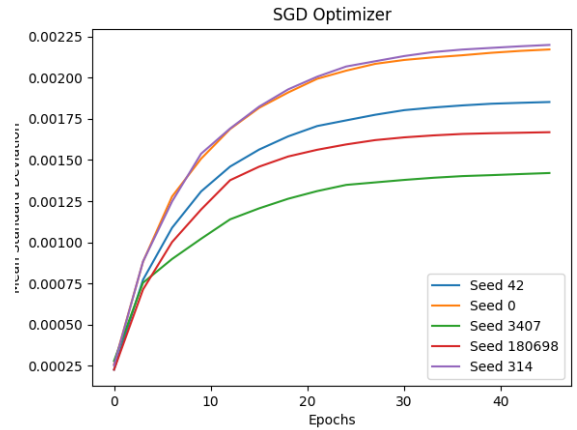
(c) CBIS-DDSM Variances for ADAM Optimizer



(d) CBIS-DDSM Variances for SGD Optimizer



(e) SDNET Variances for ADAM Optimizer



(f) SDNET Variances for SGD Optimizer

Fig. 4: Mean standard deviation plots with respect to epoch number for each optimizer and dataset across five different seed configurations. The figures display the mean standard deviation in the classification head for each model and its progression over the training course. The comparison between the SGD and ADAM optimizers is highlighted for three datasets: CIFAR-10, CBIS-DDSM, and SDNET. The plots reveal the trends in standard deviations, showcasing how the randomness introduced by CUDA affects the consistency of model performance. Notably, the figures demonstrate how certain seed values contribute to greater fluctuations, with the ADAM optimizer often exhibiting more pronounced variances compared to SGD, particularly in the later epochs.